The Ozone Monitoring Instrument

Pieternel F. Levelt, Gijsbertus H. J. van den Oord, Marcel R. Dobber, Anssi Mälkki, Huib Visser, Johan de Vries, Piet Stammes, Jens O. V. Lundell, and Heikki Saari

***Abstract*—The Ozone Monitoring Instrument (OMI) flies on the National Aeronautics and Space Adminsitration's Earth Observing System Aura satellite launched in July 2004. OMI is a ultraviolet/visible (UV/VIS) nadir solar backscatter spectrometer, which provides nearly global coverage in one day with a spatial resolution of 13 km × 24 km. Trace gases measured include O_3, NO_2, SO_2, HCHO, BrO, and OClO. In addition, OMI will measure aerosol characteristics, cloud top heights, and UV irradiance at the surface. OMI's unique capabilities for measuring important trace gases with a small footprint and daily global coverage will be a major contribution to our understanding of stratospheric and tropospheric chemistry and climate change. OMI's high spatial resolution is unprecedented and will enable detection of air pollution on urban scale resolution. In this paper, the instrument and its performance will be discussed.**

***Index Terms*—Air quality, atmospheric research, ozone layer, ultraviolet/visible (UV/VIS) satellite instruments.**

I. Introduction

THE Ozone Monitoring Instrument (OMI), a contribution of The Netherlands and Finland to the National Aeronautics and Space Adminsitration' (NAS) Aura mission, is flown on the Aura spacecraft. Aura is part of the NASA's long-term Earth Observing System (EOS) mission and was launched July 15, 2004, from Vandenberg Air Force base in California. The Aura spacecraft circulates in a 98.2° inclination, sun-synchronous polar orbit at 705-km altitude, with a local afternoon equator crossing time at 13:45 (ascending node), providing 14 orbits a day. The mission has a design lifetime of five years once in orbit. The Aura spacecraft also carries three other instruments: the Microwave Limb Sounder (MLS) [1], the High Resolution Dynamics Limb Sounder (HIRDLS) [2], and Tropospheric Emission Spectrometer (TES) [3]. MLS and HIRDLS are limb sounding instruments. TES has both limb sounding and nadir sounding modes.

Manuscript received May 20, 2005; revised October 7, 2005. This work was supported in part by The Netherlands Agency for Aerospace Programmes (NIVR).

P. F. Levelt, G. H. J. van den Oord, M. R. Dobber, and P. Stammes are with the Royal Dutch Meteorological Institute (KNMI), KS/AS, 3730 AE De Bilt, The Netherlands (e-mail: llevelt@knmi.nl; oordvd@knmi.nl; dobber@knmi.nl; stammes@knmi.nl).

A. Mälkki is with Geophysical Research, Finnish Meteorological Institute, Earth Observation, FIN-00101 Helsinki, Finland FIN-00101 Helsinki, Finland (e-mail: Anssi.Malkki@fmi.fi).

H. Visser is with Netherlands Organisation for Applied Scientific Research TNO-TPD, NL 2600 AD Delft, The Netherlands (e-mail: hvisser@tpd.tno.nl).

J. de Vries is with Dutch Space BV, NL 2303 DB Leiden, The Netherlands (e-mail: j.de.vries@dutchspace.nl).

J. O. V. Lundell is with Patria Finavitec Oy Systems, FIN-33100 Tampere, Finland (e-mail: jens.lundell@patria.fi).

H. Saari is with VTT Automation, FIN-02044 VTT, Finland (e-mail: heiki.saari@vtt.fi).

Digital Object Identifier 10.1109/TGRS.2006.872333

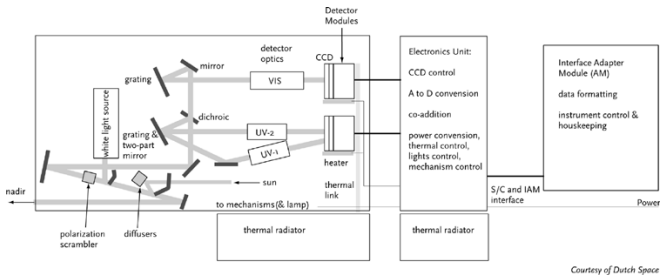

Fig. 1. Conceptual design of OMI with the large field of view out of the plane of the paper. The OMI instrument is composed of the following three elements: 1) Optical Assembly, consisting of the Optical Bench (OPB), two Detector Modules, and Thermal Hardware; 2) the Electronics Unit , performing CCD readout control and analog-to-digital conversion; 3) Interface Adaptor Module, performing Command Buffering as well as the data formatting and satellite bus interface functions.

OMI is a heritage instrument of the European Global Ozone Monitoring Experiment (GOME) [4] and Scanning Imaging Absorption Spectrometer for Atmospheric Chartography (SCIAMACHY) instruments [5], which introduced the concept of measuring the complete spectrum in the ultraviolet/visible/near-infrared (UV/VIS/NIR) wavelength range with a high spectral resolution. This enables one to retrieve several trace gases at the same time for the same air mass. The American predecessor of OMI is NASA's Total Ozone Mapping Spectrometer (TOMS) instrument. TOMS uses a different retrieval algorithm with only six wavelength bands, from which the ozone column can be obtained very accurately [6]. TOMS has the advantage that it has a fairly small ground-pixel size (50 km × 50 km) in combination with a daily global coverage. OMI combines the advantage of GOME and SCIAMACHY with the advantage of TOMS, measuring the complete spectrum in the UV/VIS wavelength range with a very high spatial resolution (13 km × 24 km) and daily global coverage. This is possible by using a two-dimensional (2-D) detector, as has been used, for example, in the GOMOS satellite instrument [7] in comparable wavelength ranges. The small pixel size enables OMI to look "in between" the clouds, which is very important for retrieving tropospheric information [8].

OMI was built by Dutch Space and TNO TPD in The Netherlands in cooperation with Finnish VTT and Patria Advanced Solutions Ltd. The Royal Netherlands Meteorological Institute (KNMI) is the Principal Investigator Institute. Overall responsibility for the OMI mission lies with The Netherlands Agency for Aerospace Programmes (NIVR) with the participation of the Finnish Meteorological Institute (FMI).

II. Measurement Technique

UV/VIS spectrometers detect the solar irradiance scattered and absorbed by the constituents of the Earth atmosphere. For

TABLE I
SPECTRAL PERFORMANCE RANGE, SPECTRAL RESOLUTION, SAMPLING DISTANCES, AND DATA PRODUCTS

Channel	*Total range*	*Full performance range*	*Average Spectral resolution (FWHM)*	*Average Spectral sampling distance*	*Data products*
UV-1	270 – 314 nm	270 – 310 nm	0.42 nm	0.32 nm/pixel	O_3 profile, O_3 column (TOMS), Surface UV-B
UV-2	306 – 380 nm	310 – 365 nm	0.45 nm	0.15 nm/pixel	O_3 profile, O_3 column (TOMS & DOAS), BrO, OClO, SO_2, HCHO, Aerosol, Surface UV-B, Surface Reflectance, cloud top pressure, cloud cover
VIS	350 – 500 nm	365 – 500 nm	0.63 nm	0.21 nm/pixel	NO_2, Aerosol, OClO, Surface UV-B, Surface Reflectance, cloud top pressure, cloud cover

retrieving atmospheric trace gases in the UV/VIS wavelength range, it is therefore essential to measure the Earth radiance and solar irradiance spectrum, the latter serving as reference spectrum for the radiance spectrum. By normalizing the radiance spectrum by the solar irradiance spectrum, the reflectance spectrum is obtained, which is used as the primary spectrum for retrieval of the atmospheric trace gases. The reflectance R is defined as $R = \pi I/(\mu_o E)$, where I is the Earth radiance, E the solar irradiance, and μ_o the cosine of the solar zenith angle. In the reflectance spectrum the strong solar Fraunhofer lines are removed and do not mask the small absorption features of the trace gases. However, due to the Raman scattering effect (also called the Ring effect [9], [10]), that effectively broaden the Fraunhofer lines and all atmospheric absorption lines in the radiance spectrum, small spectral features remain in the reflectance spectrum. These should be taken into account in the retrieval. All retrieval algorithms start from the reflectance spectrum. It is therefore important to accurately calibrate the reflectance, for which an accurate calibration to the 1% level of the so-called bidirectional scattering distribution function (BSDF) of the OMI instrument is needed [11]. The ratio of the calibrated radiance and irradiance is the Earth atmospheric BSDF. The ratio of the OMI radiance and irradiance calibration functions equals the BSDF of the instrument, for which the onboard diffuser is the most important contributor. The ratio of the radiometrically uncalibrated radiance and irradiance signals as measured by the instrument in electrons per second equals the ratio of the Earth atmospheric BSDF and the OMI instrument BSDF [11]. During the on-ground calibration phase the Earth atmospheric BSDF is replaced by the BSDF of an accurately calibrated external spectralon diffuser plate. In this way, the OMI instrument BSDF is calibrated against the known spectralon diffuser BSDF. In orbit, the unknown Earth BSDF is subsequently calibrated against the known OMI instrument BSDF. The BSDF calibration was performed prelaunch and will be further improved using in-flight measurement data. The obtained results and methods used for the on-ground calibration are extensively discussed in Dobber *et al.* [11]. A detailed overview of all in-flight calibration results is outside the scope of [11] and will be described in a future publication. To detect the radiance and irradiance, OMI uses a 2-D charge-coupled device (CCD) detector, one for each channel. One dimension is used to detect the spectral information, the additional dimension to obtain the spatial information. Therefore, as opposed to GOME, SCIAMACHY, and TOMS, OMI does not use a scan mirror to obtain the across track spatial information, but a large field of view (114°), which is focused on the two-dimensional detector with an innovative optical design. This enables OMI to measure the complete atmosphere with daily global coverage and at the same time obtain highly resolved spatial information. The use of 2-D detectors and the accompanying optics is probably the most innovative aspect of this instrument, which sets out a new area of UV/VIS satellite instruments. Another innovative aspect is the fact that OMI uses a polarization scrambler, which depolarizes the radiation over the complete wavelength range, as opposed to GOME and SCIAMACHY, which are polarization sensitive instruments. In Fig. 1, a schematic overview of the OMI instrument is given. OMI consists of three parts: an optical assembly, including the optical bench and the detector modules, the electronics unit, and the interface adaptor module. Hereafter, several important aspects of UV/VIS instruments in relation to requirements resulting from retrieval techniques and their impact on the design of OMI will be discussed.

A. OMI's Spectral Channels

OMI measures the reflected solar radiation in the ultraviolet and visible part in the spectral range that is between 270 and 500 nm, using two channels with a spectral resolution of about 0.5 nm. The light entering the telescope is spatially pseudodepolarized using a scrambler and then split in two channels: the UV channel (full performance range 270–365 nm) and the VIS channel (full performance range 365–500 nm). The UV channel consists of two subchannels with the following full performance ranges: the UV-1, ranging from 270–310 nm, and the UV-2 ranging from 310–365 nm. The spectral and spatial sampling of the UV-1 are reduced by a factor of two compared to the UV-2. The full performance range of the VIS-channel ranges from 365–500 nm. The full performance and spectral wavelength ranges, spectral sampling distances and spectral resolutions can be found in Table I. Table I also gives an overview of the gases that can be retrieved from OMI measurements. In Figs. 2 and 3, the radiance and irradiance optical paths of OMI are described.

B. OMI Electronics

The OMI electronics consists of two identical Detector Modules (DEMs), housing the CCD detectors, and the Electronics Unit (ELU), providing control and data interface toward the spacecraft. For understanding the data these functions are secondary, and so only a brief description of the units is given here.

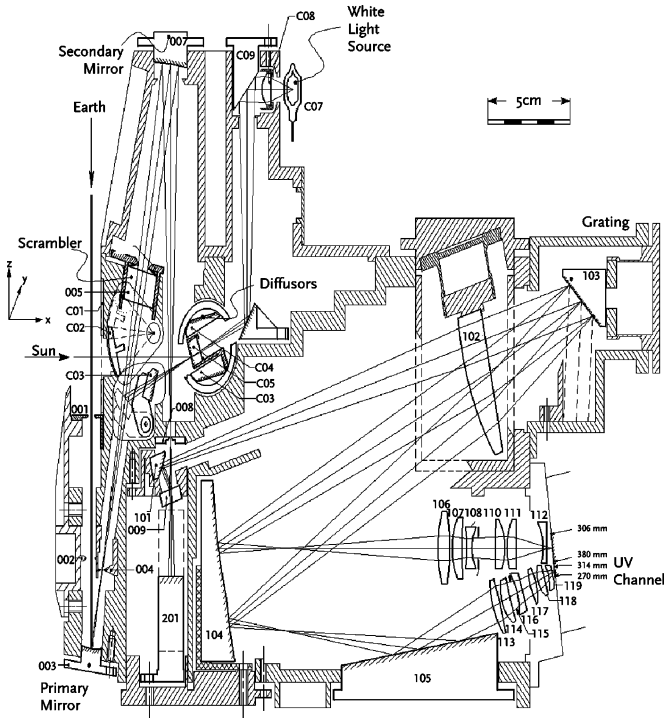

Fig. 2. Optical layout of the telescope, UV-1 and UV-2 channel and the calibration optics (Courtesy of TNO-TPD). Optical Path Description: Telescope. The telescope has a wide field of view of 114°, which enables daily global coverage at the equator. It uses for that a wide field reflective telecentric configuration. The telescope consists of two spherical mirrors (103 and 007). Radiation from the Earth is imaged on the entrance slit (008) of the spectrometer. Between the primary and secondary mirror a polarization scrambler (005) is positioned. The large field of view 114° is in the plane perpendicular to the plane of drawing. The secondary mirror (007) has a coating to suppress stray light from 500 nm up toward longer wavelengths, and to reduce the light flux for the visible channel. UV channel. Behind the entrance slit (008) a dichroic mirror (009) reflects the spectral range of the UV channels to folding mirror (101) and transmits the VIS spectral range to a flat mirror (201), that reflects the light at 90° out of the plane of drawing. The UV radiation is reflected by mirror (101) to a plano convex fused silica lens (102) that collimates the beam from the entrance slit in the direction of the grating (103). The function of the collimating/imaging lens (102) is twofold: it creates a parallel incoming beam on the grating (103) and forms an intermediate spectrum of the diffracted beams close to the field mirror (104). The grating (103) is used in the first order. An intermediate UV spectrum is created, close to a (split) field mirror (104). This field mirror is supplied with a coating with a wavelength (= position) dependent variable reflection in order to suppress the stray light of larger wavelengths in the extreme UV. Depending on the bandwidth of reflection coating (at each position), a suppression of stray light of one order of magnitude is reached. The UV-1 image is scaled down by a factor of 2 on the CCD compared to the UV-2 image, in order to improve the S/N performance of the UV-1 channel by a factor of square root (2), at the cost of doubling the ground pixel size in the swath direction.

1) ELU: The ELU handles the electronics of the OMI instrument. The ELU regulates and provides power and control for the instrument. On the other hand, the ELU connects to the satellite via the Instrument Adapter Module (IAM) through which all instrument commands and data are transmitted.

The ELU has two video channels, one for controlling the exposure times and readout of each CCD, processing and converting the analog video signals to digital samples, formatting these into fixed length packets and periodically transmitting the packets toward the IAM. The operation of instrument heaters, as well as any operations needed for calibration measurements (such as light sources, movement of diffusers etc.) are also controlled by the ELU.

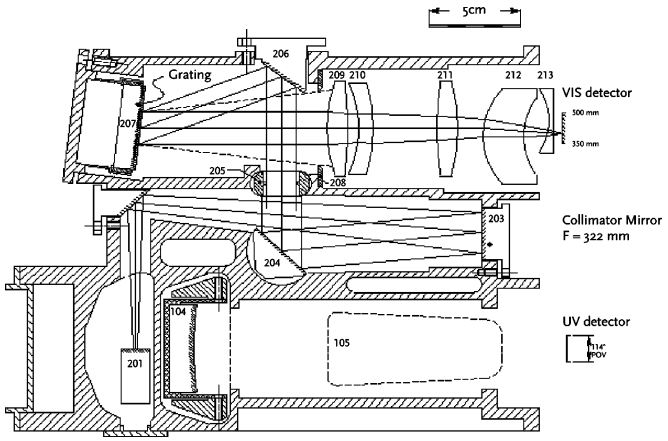

Fig. 3. Optical layout of the visible channel (Courtesy of TNO-TPD). VIS channel. Note that the orientation of the plane of drawing of Fig. 4 is perpendicular to that of Fig. 3. The "visible" part of the spectrum (350 – 500 nm) is reflected by mirror (201) via folding mirror (202) to a collimating mirror (203). The rest of the visible channel is rather straight forward and consists of 2 folding mirrors (204 and 206), a plane grating with 1350 gr/mm (207) and an objective (209–213) to image the diffracted beams on the second detector.

2) DEMs: After the optics, the first part down the signal flow is the CCD, which is discussed more in detail in other parts of this paper. The Detector Module provides the housing to the CCD, including thermal control. It translates the CCD readout sequence (provided by the ELU) to CCD input and clock signals, reads out the CCD pixel voltages, provides preamplification to the CCD signal based on gain settings defined by the ELU and sends the resulting analog video signals to the ELU.

C. Observation Modes

Apart from highly resolved spectral information, OMI's largest asset is the obtained high spatial resolution, combined with daily global coverage. The spatial resolution of OMI is unprecedented for UV/VIS satellite instruments. The nadir pointing telescope of OMI has a very large field of view of 114°, which is used for swath registration, perpendicular to the flight direction of the satellite. Due to this wide field of view of 114°, the OMI swath width is 2600 km, which provides, combined with 14 orbits a day, daily global coverage. The use of 2-D CCD detectors enables to measure the spectral and spatial information at the same time. One dimension of the CCD (780 pixels) is used to cover the spectrum, the other direction (576 pixels) is used to cover the viewing direction, as illustrated in Fig. 4. The OMI CCD has an UV enhanced detection, using a special coating which increases the detector UV quantum efficiency with 30% [11], to realize a high quantum efficiency especially in the UV. Pixel full well is 300 000 electrons (see [11] for more details on the detector).

The main observation mode for OMI is the Global measurement mode. OMI can measure in two additional modes: the Spatial zoom-in measurement mode and the Spectral zoom-in measurement mode (see Table II). In a regular OMI Earth radiance measurement, five measurements with an exposure time of 0.4 s are co-added, resulting in a pixel size in the flight direction of 13 km, independent of the operation mode. Also other exposure times are used; however, the total effective integration time of an exposure remains always 2 s. The nominal exposure time is

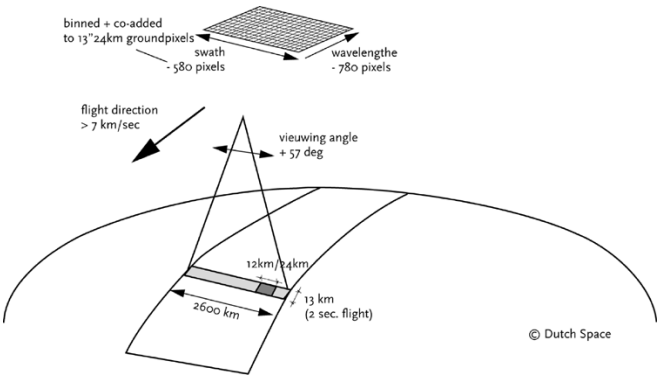

Fig. 4. OMI measurement principle.

optimized between having sufficient signal in the UV-1 channel and preventing saturation in the VIS channel.

The Global Measurement mode is the default mode and samples the complete swath of 2600 km for the complete wavelength range. The ground pixel size at nadir position in the Global mode is 13 km × 24 km (along × across track) for the UV-2 and VIS channels, and 13 km × 48 km for the UV-1 channel.

In the Spectral and Spatial zoom-in modes the ground pixel size is reduced to 13 km × 12 km for the UV-2 and VIS, and 13 km × 24 km for the UV-1. Hence, in the zoom-in modes the ground pixel size in the across track direction is reduced by a factor of two. In the Spatial zoom-in mode the complete wavelength range is available, but for the UV-2 and VIS channels the swath is reduced to 725 km. For the UV-1 the complete swath is available. In the Spectral zoom-in mode the complete swath is available, but the wavelength range is limited to 306 – 432 nm. Thus, in Spectral zoom-in mode the UV-1 is not available, and only the shorter wavelengths of the VIS channel are available. This enables retrieval of ozone, HCHO, SO_2, BrO, and OClO and aerosols at high spatial resolution of 13 km × 12 km with daily global coverage (as opposed to the spatial zoom-in mode where daily global coverage is not obtained). The Spatial zoom-in mode is used for one day per month. The Spectral zoom-in mode is not used on a regular basis.

The pixel-size in the swath-direction increases slowly from 13 km × 24 km (exact nadir position) to about 13 km × about 150 km for the global mode at the most outer swath-angle (57°). This effect is illustrated in Fig. 5.

The geolocation is required to be known to 1/10 of a ground pixel [12] for the zoom-in modes. This requirement was verified by generating RGB pictures of OMI measurements. In Fig. 6, an RGB picture is shown, which was used for geolocation verification. Also a super zoom-in mode was defined for geolocation calibration. In this mode a spatial sampling can be achieved of about 3 km × 3 km.

D. Calibration

In addition to the nominal operational mode, OMI will also perform in-flight calibration measurements. The most important in-flight calibration measurement is the observation of the Sun. Once per day, OMI observes the Sun by opening the Sun aperture and rotating a folding mirror and a diffuser in the light path. Three diffusers are available for solar measurements. To monitor the overall performance of the instrument, OMI has

TABLE II
CHARACTERISTICS OF THE MAIN OBSERVATION MODES

Channel	*Spectral range [nm]*	*Swath width [km]*	*Ground pixel size* [a] *[km]*	*Application / operational frequency*
Global Observation Mode				
UV-1	270 – 310	2600	13 × 48	global observation of all products / *daily*
UV-2 & VIS	350 – 500	2600	13 × 24	
Spatial Zoom-in Observation Mode				
UV-1	270 – 310	2600	13 × 24	regional studies of all products / *about one day per month*
UV-2 & VIS	350 – 500	725	13 × 12	
Spectral Zoom-in Observation Mode				
UV-2	306 – 364	2600	13 × 12	global observation of some products / *special occasions*
VIS	350 – 432	2600	13 × 12	

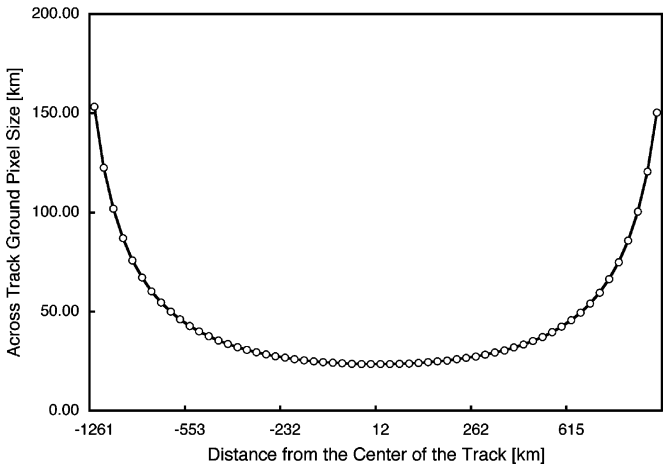

Fig. 5. OMI ground pixel size in the swath direction as a function of distance from the nadir position.

an internal White Light Source (WLS). The WLS is observed via a transmission diffuser. To separately check the sensitivity of the CCD pixels, there are also light emitting diodes (LEDs) available.

The white light source (C07 in Fig. 3) is a tungsten halogen lamp with a quartz bulb. The WLS is used to monitor and determine the radiometric degradation, the pixel-to-pixel variation and the nonlinearity of the detector.

Two LEDs, emitting in the green, are positioned close to the CCD-detector. The primary use of the LEDs is identification of bad pixels, to obtain the relative electronic gain values and nonlinearity parameters of the electronics.

The WLS is operated once per week, the LEDs once per day.

During the on-ground calibration effort the following calibration parameters have been measured: absolute radiance, absolute irradiance, instrument BSDF, including their swath angle dependences, spectral knowledge and stability, slit function as a function of wavelength and swath angle, viewing properties, stray light, overall polarization dependence, diffuser characteristics, detector and electronics characteristics. An extensive paper on the calibration of the OMI instrument can be found in this IEEE special issue [11] as well as information on the OMI operational concept [13].The measurements and

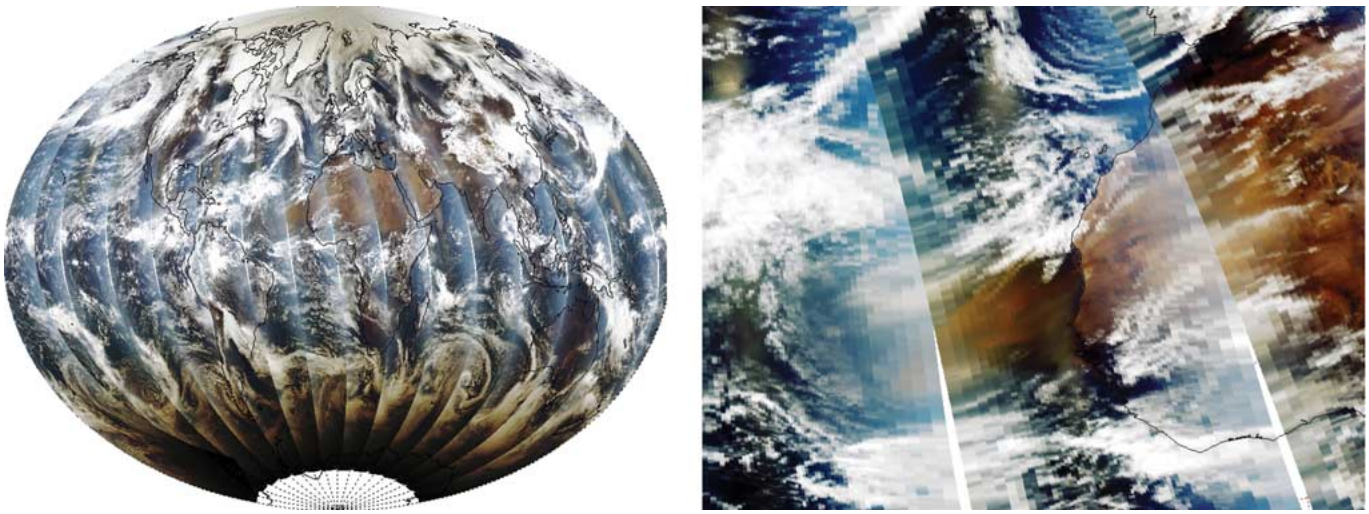

Fig. 6. RGB plot for one day of OMI measurements on May 16, 2005. Dust storm and its outflow can be seen above the Sahara dessert.

methods used and their analyses results are described in paper [11] and [13].

III. Retrieval Techniques

The OMI data products as shown in Table I are obtained using different retrieval techniques (see Table III). The algorithms heavily depend on experience gained from TOMS, SBUV, GOME, and SCIAMACHY. There are roughly five major retrieval techniques used: TOMS type of retrieval (Ozone column, SO_2), DOAS type (O_3, NO_2, O_2-O_2 (cloud pressure), HCHO, OClO, and BrO), optimal estimation methods (Ozone profile), Raman scattering (cloud pressure), and retrievals based on changes in the reflectance over long wavelength ranges (aerosols). In a companion paper in this special issue describing the Science Objectives of the OMI instrument [8], the algorithms for the standard products are described. References for detailed description are included. Depending on the retrieval technique the dependence on the performance and calibration aspects of the OMI instrument is different. Since DOAS retrieval is dependent on a successful discrimination of small highly spectrally dependent absorption features, it is sensitive to the *spectral calibration*, the *spectral stability*, and *spectrally dependent features* of the instrument. Also the cloud retrieval via the Raman scattering technique is sensitive to these spectral issues. Due to the temperature difference over an orbit, the radiance and irradiance spectra will slightly shift over the CCD detector pixels. The spectral stability of OMI reflects the requirement on how large this shift is allowed to be within one orbit. In the spectral wavelength determination used for OMI, accurate knowledge of the *spectral slit function* is also essential. TOMS-type of retrieval, ozone profile, and aerosol and cloud fraction retrievals are less sensitive to spectral characteristics of the instrument, but are sensitive to the *absolute calibration of the reflectance*, and thus to the instrument BSDF, with an increased sensitivity toward larger wavelength ranges used. Particularly ozone profile retrieval, based on the large change of absorption by the Hartley and Huggins bands of ozone in the UV-1 wavelength range (270–310 nm), is sensitive to the absolute calibration, due to the large wavelength range used, and the fact that in this wavelength range the reflectance changes with three orders of magnitude, with resulting low signal to noise at the short wavelength side. *Stray light* from higher wavelengths in the 270–290-nm interval can also significantly interfere with the ozone profile retrieval. Aerosol retrieval is also dependent on the use of a large wavelength range and particularly sensitive to the presence of clouds and surface albedo. Cloud fraction and surface albedo are also dependent

TABLE III
(a) OMI Algorithms in the UV-1 Channel. (b) OMI Algorithms in the UV-2 Channel. (c) OMI Algorithms in the VIS Channel. Col. = Column amounts (V = Vertical; S = Slant column) TOMS Wavelengths Are Used for TOMS O_3, SO_2 (V) Column, Aerosol Index, and Aerosol Optical Depth Products. An Overview Is Given of the Wavelength Bands That Are Used for OMI Level 2 Data Products

Product name	*Col.*	*Wavelength Band [nm]*	*Algorithm*
O_3 Profile	--	270 – 314	Optimal estimation
TOMS#5 312.5	V	311.5 – 313.5	TOMS
TOMS#6 308.6	V	307.5 – 309.5	TOMS
Surface UV irradiance	--	280 – 314	Reflectance change
O_3 column	V	325 – 335	DOAS
O_3 Profile	--	306 – 314	Optimal estimation
Aerosol	V	340 – 365	Reflectance change
BrO column	S	344 – 360	DOAS
SO_2 column	V	310 – 331	Pair Algorithm
OClO column	S	357 – 381	DOAS
HCHO column	V	336 – 357	DOAS
Surface UV irradiance	--	306 – 380	Reflectance change
TOMS#1 360.0	V	359 – 361	TOMS
TOMS#2 331.2	V	330.2 – 332.2	TOMS
TOMS#3 322.3	V	321.3 – 323.3	TOMS
TOMS#4 317.5	V	316.5 – 318.5	TOMS
TOMS#5 312.5	V	311.5 – 313.5	TOMS
TOMS#6 308.6	V	307.5 – 309.5	TOMS
NO_2 column	V	425 – 450	DOAS
Cloud Top Pressure (Raman)	--	390 – 400	Raman scattering
Cloud Cover	--	378 – 383	Reflectance change
Cloud Top Pressure (O_2- O_2)	--	460 – 490	DOAS
O_3 Profile	--	350 – 500	Optimal estimation
Aerosol	V	350 – 500	Reflectance change
OClO column	S	357 – 381	DOAS
Surface UV irradiance	--	350 – 400	Reflectance change
TOMS#1 360 nm	V	359 – 361	TOMS

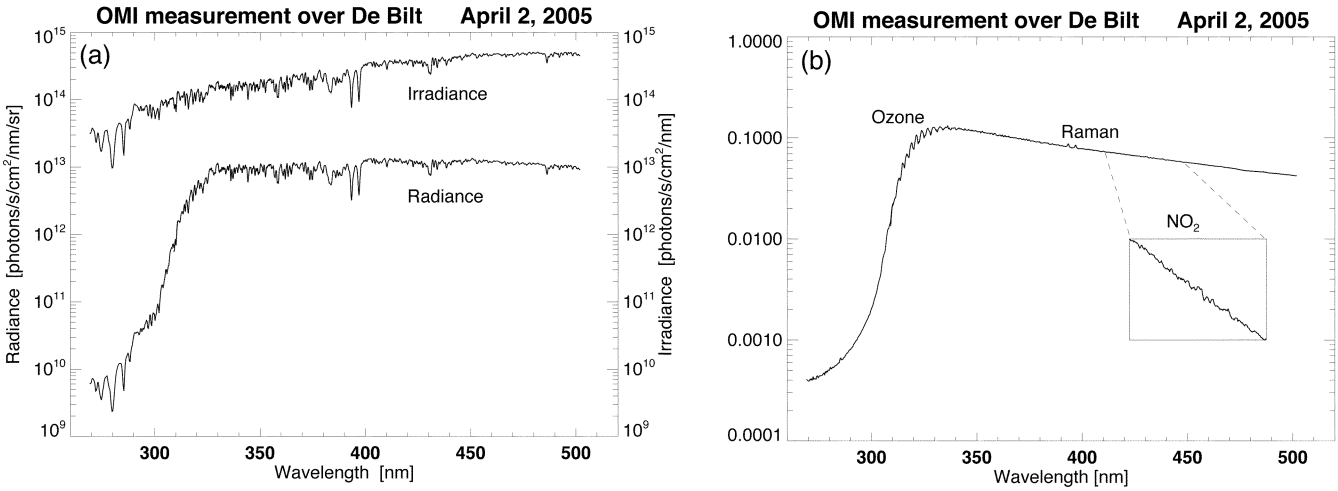

Fig. 7. (a) OMI solar irradiance and Earth radiance spectrum above The Netherlands on a cloudless day (April 2, 2005). (b) Ratio spectrum of the radiance and irradiance spectra of (a). Absorption peaks of ozone Hartley and Hugging bands are clearly visible between 270 and 330 nm. The double peak around 390 nm are the Raman lines from the Calcium Fraunhofer lines. Between 410 and 450 nm the tiny absorption features of NO_2 are visible.

on the absolute reflectance. In the TOMS–type of retrieval (total ozone, SO_2 index and aerosol index), based on the use of a few wavelength bands of 1 nm over a wavelength range of 308–360 nm, the absolute reflectance is also an essential factor for its accuracy. For accurate retrieval of all data products based on the reflectance, monitoring the degradation of the reflectance during instrument lifetime is mandatory. Since several optical elements in the instrument are highly *polarization* sensitive, the polarization state of the incoming radiation should be known, in order to be able to derive the correct amount of trace gas. This is the approach taken for GOME and SCIAMACHY (see e.g., [14]). However, another way to circumvent this is to pseudo-depolarize the radiation before it hits any polarization sensitive element in the instrument. In the case of OMI, this was done by using a scrambler (15; see [11] for more details). This paper will discuss above aspects of the OMI instrument that are related to the retrieval.

IV. Instrument Specifics

The accuracy of the retrieved products will contain a random component and a systematic bias which are due to instrumental effects and the retrieval method used for a particular product. The random component will be called the precision. The random component due to instrumental effects is determined by the signal-to-noise while the random component due to retrieval is caused by uncertainty in the model parameters used in the retrieval. Usually one wants to reduce the instrumental effects so that the final accuracy is dominated by the bias and precision in the retrieval algorithm. Further improvement in the retrieval algorithms during the life time of the instrument can then improve the products. In this section the instrumental effects will be considered. Retrieval algorithm effects have been described in the OMI ATBD (http://www.knmi.nl/omi/research/documents). In Fig. 7, a typical measured solar irradiance spectrum, earth radiance spectrum and their ratio spectrum, are given. Typical signal-to-noise values for OMI are 1000 to 1500 in the visible, around 1000 in the UV-2, and between 50 and 100 in the UV-1. In the following various instrumental systematic effects will be discussed.

A. Absolute Calibration of Reflectance

By dividing the radiance by the irradiance spectrum the assumption is that any specific instrument characteristics or degradation effects cancel out. In OMI the primary mirror is not shared between the Earth radiance and solar irradiance measurement, as well as the mesh, diffuser and folding mirror needed to measure the solar irradiance spectrum. The mesh is needed to reduce the intensity of the solar irradiance and prevent detector saturation and has a suppression factor of 10%. The solar irradiance is measured by opening the Solar Aperture Mechanism (SAM). The solar irradiance passes a mesh and is reflected by one of the three reflection diffusers in the Diffuser Carousel into the optical path of the telescope by reflecting from a mirror mounted in the Folding Mirror Mechanism (FMM), the third mechanism in OMI, which at the same time closes the optical path for the Earth radiances. A solar calibration measurement has therefore a different optical path from the Earth radiation measurement, adding the mesh, the reflection diffuser and the FMM mirror, and missing the primary mirror (003). The philosophy is that the FMM and the primary mirror, being made of the same material, will have a comparable degradation. To monitor the degradation of the diffuser, 3 reflection diffusers are used with a different frequency. One diffuser is used for the daily solar calibration, one diffuser is measured every week and one every month. When not used the solar port is closed using the Solar Aperture Mechanism (C02 in Fig. 2). To check the assumption above, in orbit radiance measurements under well-known atmospheric conditions and surfaces can be used as well as comparisons between solar irradiance measurements with different diffusers and solar measurements from other sources [11], [16].

B. Stray Light

Reducing stray light is one of the challenges in UV/VIS spectrometers, especially for the part of the spectrum below 290 nm, from which part of the ozone profile information originates.

Stray light can be produced spectrally (i.e., spillover from other wavelengths, e.g., VIS stray light in the UV part of the spectrum) and spatially (e.g., spillover from light with the same frequency, but produced by a different geo-location/air mass). To suppress stray light originating from above 500 nm, the secondary mirror in the telescope [(007) in Fig. 3] has a coating in order to suppress stray light from above 500 nm.

The optical design of the UV channel is optimized to reduce stray light below 290 nm. Within the UV spectral range the variation in radiance from the Earth between the shortest wavelength ($\lambda < 290$ nm) and the longer wavelength ($\lambda > 320$ nm) varies by more than three orders of magnitude. Without proper optical design the stray light at wavelengths below 290 nm exceeds the signal itself. This stray light originates from wavelengths between 310–380 nm. To avoid an excess of stray light below 290 nm, the UV channel is split into two subchannels: UV-1 and UV-2.

An intermediate UV spectrum is created, close to a (split) field mirror (104). This field mirror is supplied with a coating with a wavelength (= position) dependent variable reflection in order to suppress the stray light of larger wavelengths in the extreme UV. Depending on the bandwidth of reflection coating (at each position), a suppression of stray light of one order of magnitude is reached. Moreover by splitting the spectral range in two parts, the stray light that is caused by internal reflections in the UV-2 imaging objective, has no effect on the UV-1 spectrum at the detector surface.

The UV-1 image is scaled down by a factor of 2 on the CCD compared to the UV-2 image, in order to improve the S/N performance of the UV-1 channel by a factor of $\sqrt{2}$, at the cost of doubling the ground pixel size in the swath direction.

By the above actions, the spectral stray light below 290 nm in OMI was successfully suppressed to 1% at 270 nm after correction. This was done with measurements using bandpass and high pass filters. Subsequently a polynomial fit is obtained through the spectral stray light in the 270–290-nm region for each source region above 290 nm. This information was then used in the correction algorithm [11], [13].

C. Spectral Calibration, Stability, and Slit Function

OMI is not equipped with a spectral lamp onboard, and uses the spectrally well-known Fraunhofer lines for the spectral calibration. For the DOAS retrievals the wavelength assignment has to be known to 1/100th of a detector pixel. It has been shown that by using the Fraunhofer lines this wavelength accuracy can be obtained [11]. For obtaining the reflectance spectrum the radiance and irradiance spectra have to be interpolated to the same wavelength grid. Due to Doppler shifts and temperature changes over an orbit, the radiance and irradiance spectra do not correspond to exactly the same detector pixels [17]. Spline interpolation is not sufficiently accurate. However, because we know the spectral fine-structure of the solar irradiance, we can use this knowledge to develop a more accurate interpolation procedure. Moreover, it should be noted that it is not possible to calibrate every single spectrum using the Fraunhofer lines, since this would be too time-consuming. Therefore, the behavior of spectral shifts along the orbit are parameterised, and the spectral calibration using the Fraunhofer lines is only done for the nadir row. Therefore, the spectral stability of the OMI instrument should be 1/20th of a detector pixel, to prevent any noticeable error due to the interpolation between the radiance and irradiance spectra and to be able to use the above described parameterization.

In order to fit the Fraunhofer lines and the trace gas absorption features from the Earth's atmosphere and to perform the interpolation with the spectrally high resolved solar spectrum, accurate knowledge of the spectral slit function of the instrument as a function of wavelength and swath angle is required. A dedicated optical stimulus was developed and employed for the OMI program in order to measure these spectral slit functions accurately on the ground [18]. In-flight these slit functions will be further improved where possible [11].

D. Spectral Features

Spectral instrument features can be notorious for retrieval techniques using specific spectrally dependent absorption features, such as the DOAS method. The instrument features interfere with the specific characteristic absorption features of trace gases and reduce the accuracy of the retrieval. The stronger the features are, and the more the wavelength dependence resembles the absorption wavelength dependence, the more inaccurate the retrieval becomes. Generally speaking instrumental spectral features should remain smaller than 10^{-4} (0.01%) of the reflectance. This requirement can in some cases be relieved up to the 10^{-3} (0.1%) level, depending on the trace gas involved and the exact form of the instrument features. In OMI there are four potential sources of this kind of spectral instrument features, the scrambler, the diffusers, gratings, and the dichroic mirror. The gratings were designed and employed in such a way that no spectral features result. Concerning the dichroic mirrors the wavelength range is chosen such that it does not interfere with any of the absorption characteristics of the targeted trace gases. That leaves the scrambler and the diffusers.

The scrambler features have been extensively measured on-ground. The features change with wavelength in intensity and frequency, with increasing intensity and slower wavelength variation toward larger wavelengths. The measurements were used to determine the amount of interference with the retrieval of trace gases using a DOAS-type of retrieval, i.e., total ozone, NO_2, HCHO, OClO, and BrO. These prelaunch simulations showed that the scrambler features interference did not add an extra error to the retrieved trace gases, on top of the errors caused by other instrument characteristics or retrieval errors. This was expected since the scrambler features do have a broader wavelength dependence than the absorption features of the trace gases and therefore have a limited effect on DOAS type of retrievals.

The amplitude and frequency pattern of the diffuser features strongly depend on the specific diffuser used. In OMI we have three types of diffusers: a transmission diffuser used for the internal White Light Source measurement, and two types of reflection diffusers, one Quartz Volume Diffuser used for the daily solar measurements, and two aluminum diffusers used for the weekly and monthly solar calibration measurements. For the retrieval the reflectance spectrum is used. In the solar irradiance spectrum the reflection diffuser features are present. The transmission diffuser features are present in a WLS measurement, used to determine the

in-flight Pixel Response Non Uniformity (PRNU) map for the detectors, in order to correct the measured Earth radiance and solar irradiance intensities on detector pixel level. The PRNU cancels out to first order in the calculated reflectance (see [11] for more details). The reflection diffuser features change in frequency and amplitude depending on the angle of the solar light as it enters the instrument, which means that they change all year round, due to different solar elevation and azimuth angles. The transmission diffuser features should stay the same, except for degradation effects. In the on-ground calibration program the features for all three types of diffusers have been partly qualitatively characterized [11]. The conclusion is that the aluminum diffuser features would be too large for successful DOAS retrieval. Those diffusers are therefore only used to check the absolute calibration, since the experience is that these types of diffusers do not degrade so fast. Therefore, a new type of diffuser, the Quartz Volume Diffuser (QVD), was specially procured and tested for OMI. Its features have an amplitude of about a factor of ten smaller than those of the Aluminum diffusers [11]. These fairly small high frequency diffuser features could still interfere with the DOAS retrieval, but do not introduce a large error due to their small amplitude. The transmission diffuser features also turned out to be sufficiently small. Nevertheless, the in-flight calibration program includes the determination of the reflection diffuser features and their degradation [11].

E. Polarization

The light reflected by the Earth atmosphere is generally polarized. Moreover, instruments like OMI are generally sensitive to the state of polarization of the light that enters the instrument, due to polarization dependent properties of mirrors, dichroics, and gratings. This dependence can in principle be corrected for if the response of the instrument is well characterized preflight with respect to the state of polarization of the incident light, and if the response is not changing in-flight. However, for OMI, we have chosen to make OMI insensitive to polarization by using a polarization scrambler (005 in Fig. 3). This has the advantage that the calibration and level 0 to 1b software takes less effort, because only one type of light enters the instrument. Moreover, for polarization-dependent instruments the absolute radiometric calibration is less accurate than for polarization-independent instruments.

The scrambler transforms one polarization state into a continuum of polarization states that effectively depolarizes the signal. However this is not equal to totally depolarized light. Therefore, the scrambler is called a pseudodepolarizer. For OMI a spatial pseudopolarizer is applied [15], which transforms the input into an output of which the polarization state varies with position over the scrambler exit aperture. Polarization effects due to the primary mirror are partly compensated for by the first scrambler surface. The overall polarization sensitivity of the instrument has been measured and turned out to be smaller than 0.5%, which agrees well with the optical design [11].

V. Conclusion

In this paper, the main instrument features of the OMI instrument in relation to retrieval requirements were discussed. The most innovative aspects of OMI, which is the use of 2-D CCD detectors in combination with an innovative optical design, as well as the use of a polarization scrambler to depolarize the radiation is described.

Acknowledgment

The authors thank R. Noordhoek and P. Veefkind for their help in putting the text and figures in the IEEE format, R. Voors for providing Fig. 7, and R. Dirksen and M. Kroon for providing Fig. 6. J. de Haan is acknowledged for his thorough reading of the manuscript and his valuable comments. The anonymous reviewers are acknowledged for there valuable comments.

References

[1] J. Waters *et al.*, "The Earth Observing System Microwave Limb Sounder (EOS MLS) on the Aura satellite," *IEEE Trans. Geosci. Remote Sens.*, vol. 44, no. 5, pp. 1075–1092, May 2006.

[2] J. Gille *et al.*, "High Resolution Dynamics Limb Sounder (HIRDLS)," JPL, Pasadena, CA, 2005.

[3] R. Beer, "TES on the Aura mission: Scientific objectives, measurements, and analysis overview," *IEEE Trans. Geosci. Remote Sens.*, vol. 44, no. 5, pp. 1102–1105, May 2006.

[4] J. P Burrows *et al.*, "The Global Ozone Monitoring Experiment (GOME): Mission concept and first scientific results," *J. Atmos. Sci.*, vol. 56, pp. 151–175, 1999.

[5] H. Bovensmann *et al.*, "SCIAMACHY—Mission objectives and measurement modes," *J. Atmos. Sci.*, vol. 56, no. 2, pp. 127–150, 1999.

[6] C. G. Wellemeyer, P. K. Bhartia, S. L. Taylor, W. Qin, and C. Ahn, "Version 8 Total Ozone Mapping Spectrometer (TOMS) algorithm," presented at the *20th Quad. Ozone Symp.*, C. S. Zerefos, Ed., Athens, Greece, 2004.

[7] E. Kyrölä, J. Tamminen, G. W. Leppelmeier, V. Sofieva, S. Hassinen, J. L. Bertaux, A. Hauchecorne, F. Dalaudier, C. Cot, O. O. Korablev, O. Fanton d'Andon, G. Barrot, A. Mangin, B. Théodore, M. Guirlet, F. Etanchaud, P. Snoeij, R. Koopman, L. Saavedra, R. Fraisse, D. Fussen, and F. Vanhellemont, *GOMOS Envisat: An Overview. Adv. Space Res.*, vol. 33, no. 7, pp. 1020–1028, 2004.

[8] P. F. Levelt, E. Hilsenrath, G. W. Leppelmeier, G. H. J. van den Oord, P. K. Bhartia, J. Tamminen, J. F. de Haan, and J. P. Veefkind, "Science objectives of the Ozone Monitoring Instrument," *IEEE Trans. Geosci. Remote Sens.*, vol. 44, no. 5, pp. 1199–1208, May 2006.

[9] J. F. Grainger and J. Ring, "Anomalous Fraunhofer line profiles," *Nature*, vol. 193, p. 762, 1962.

[10] M. Vountas, V. Rozanov, and J. Burrows, "Ring effect: Impact of rotational raman scattering on radiative transfer in Earth's atmosphere," *J. Quant. Spectrosc. Radiat. Transf.*, vol. 60, no. 6, pp. 943–961.7, 1998.

[11] M. R. Dobber *et al.*, "Ozone Monitoring Instrument calibration," *IEEE Trans. Geosci. Remote Sens.*, vol. 44, no. 5, pp. 1209–1238, May 2006.

[12] P. F. Levelt *et al.*, "Science requirements document for OMI-EOS," KNMI, de Bilt, The Netherlands, KNMI Pub. 193, RS-OMIE-KNMI-001, 2nd ed., 2000.

[13] G. H. J. van den Oord *et al.*, "OMI level 0 to 1b processing and operational aspects," *IEEE Trans. Geosci. Remote Sens.*, vol. 44, no. 5, pp. 1380–1397, May 2006.

[14] N. A. J. Schutgens and P. Stammes, "A novel approach to the polarization correction of space-borne spectrometers," *J. Geophys. Res.*, vol. 108, no. D7, 2003.

[15] J. P. McGuire and R. A. Chipman, "Analysis of spatial pseudodepolarizers in imaging systems," *Opt. Eng.*, vol. 29, pp. 1478–1484, 1990.

[16] G. Jaross, A. J. Krueger, and D. Flittner, *Metrologia*, vol. 35, pp. 625–629, 1998.

[17] J. P. Veefkind, J. F. de Haan, E. J. Brinksma, M. Kroon, and P. F. Levelt, "Total ozone from the Ozone Monitoring Instrument (OMI) using the DOAS technique," *IEEE Trans. Geosci. Remote Sens.*, vol. 44, no. 5, pp. 1239–1244, May 2006.

[18] M. Dobber, R. Dirksen, R. Voors, G. H. Mount, and P. Levelt, "Ground-based zenith sky abundances and *in situ* gas cross sections for ozone and nitrogen dioxide with the Earth Observing System Aura Ozone Monitoring Instrument," *Appl. Opt.*, vol. 44, no. 14, pp. 2846–2856, May 2005.

Pieternel F. Levelt received the M.S. degree in physical chemistry and the Ph.D. degree from the Free University of Amsterdam, Amsterdam, The Netherlands, in 1987 and 1992, respectively. Her Ph.D. work consisted of the development of a XUV spectrometer-based nonlinear optical technique and performing XUV spectroscopy on small diatomic molecules.

In 1993, she started working at the Royal Netherlands Meteorological Institute (KNMI), De Bilt, in the Atmospheric Composition section at the Research Department of KNMI. There, she worked on chemical data assimilation of ozone in two-dimensional and three-dimensional chemistry transport models and on the validation of the European satellite instruments GOME and SCIAMACHY. She was a Member of the Algorithm and Validation subgroups of GOME and SCIAMACHY. She was strongly involved in the validation program of both instruments. Since July 1998, she has been Principal Investigator of the OMI instrument and is responsible for the scientific program of OMI and managing the international OMI Science Team. She is also the Project Manager of the OMI Program at KNMI and responsible for the development of algorithms, validation, and data processing of OMI products and in-flight calibration and operational planning of the OMI instrument. She is managing the OMI team at KNMI consisting of 15 to 35 people. As Principal Investigator, she is advising NIVR on OMI instrument requirements and performance.

Gijsbertus H. J. van den Oord is currently with the Royal Dutch Meteorological Institute (KNMI), De Bilt, The Netherlands. He has a 16-year-long background in both observational and theoretical astrophysics with emphasis on solar and stellar magnetic activity. On the theoretical side, he has worked in the fields of magnetohydrodynamics, plasma physics, beam electrodynamics, high-energy astrophysics, X-ray spectroscopy, and radiative transport. On the observational side, he has been an active user of (ground-based) radio and optical instrumentation, and spaceborne X-ray and (E)UV instrumentation. He has supervised two Ph.D. students and is author and coauthor of 72 papers. Since April 1999, he has been the Deputy Principal Investigator of the Ozone Monitoring Instrument. He has been a Visiting Professor at the University of Catania. He has been a member of numerous science advisory boards on both national and international level.

Dr. van den Oord received an award from Utrecht University for outstanding research accomplishments.

Marcel R. Dobber studied experimental physics from 1990 to 1994 at the Free University of Amsterdam, Amsterdam, The Netherlands, and received the Ph.D. degree in physical chemistry from the University of Amsterdam, for work on high-resolution and time-resolved molecular laser spectroscopy.

He started working on Earth observation from space in 1995 and joined the Royal Dutch Meteorological Institute (KNMI), De Bilt, The Netherlands, in 2001, where he has been working mainly on the development and on-ground and in-flight calibration of the OMI instrument on NASA's EOS Aura satellite.

Anssi Mälkki received the Ph.D. degree in space physics from the University of Helsinki, Helsinki, Finland, in 1993.

He currently works as Research Manager at the Space Research Unit, Finnish Meteorological Institute, Helsinki. He worked at the Space Science Department of the European Space Agency, Noordwijk, The Netherlands, from 1994 to 1996. In the OMI Program, he has worked as Project Manager and Program Manager for the Finnish contribution. He is currently the coordinator of WMO-sponsored IGACO-O3 secretariat at FMI.

Huib Visser received the M.Sc. degree in physics from the Delft University of Technology, Delft, The Netherlands, in 1968.

He joined the Optics Department, Netherlands Organisation for Applied Scientific Research (TNO), Delft, in 1968 and, since then, he has been involved in the realization of many optical space instruments, among which GOME, SCIAMACHY, MIPAS, and OMI.

Mr. Visser was appointed as Senior Research Fellow of TNO in 1994 and 1999, and in 2001, he received the David Richardson Medal of the Optical Society of America

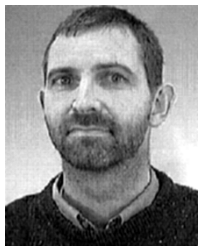

Johan de Vries has over 15 years of experience in developing spectrographs for space. He has acted as OMI Project Scientist on the industrial side from 1994 up to launch on EOS Aura in 2004. He is currently a Design Leader for future air quality instruments at Dutch Space BV, Leiden, The Netherlands.

Piet Stammes received the M.Sc. degree in physics in 1983 and the Ph.D. degree in physics and astronomy in 1989 from the Free University of Amsterdam, Amsterdam, The Netherlands.

He was a Research Fellow at ESA/ESTEC, Noordwijk, The Netherlands, from 1989 to 1991. In 1991, he became Atmospheric Research Scientist with the Royal Netherlands Meteorological Institute (KNMI), De Bilt, The Netherlands. He works on atmospheric radiative transfer modeling including polarization for the UV-visible range, with applications to calibration and retrieval of cloud and aerosol properties from the satellite spectrometers GOME, SCIAMACHY, and OMI.

Jens O. V. Lundell studied at the Tampere University of Technology, Tampere, Finland, and received the M.S. degree in electrical engineering in 1986.

Since 1992, he has worked with various space projects at Patria Advanced Solutions Oy in Finland. For the OMI instrument, he is the Project Manager for the Electronics Unit including design, manufacturing, testing, and postdelivery support.

Heikki Saari was born in Lapua, Finland, in 1954. He received the M.Sc. degree in technical physics and the Dr.Tech. degree from the Helsinki University of Technology, Helsinki, Finland, in 1980 and 1996, respectively. The subject of his doctoral thesis was "Optics, Detectors and Ground-based Star Spectra Measurements of the GOMOS Spectro-A Bench Model."

He has led several space- and airborne remote sensing instrument development projects. These include the OMI CCD Detector Modules for EOS AURA, the Scanning Micromechanical Mirror System for intersatellite optical links and Gas Sensor on the Basis of Micromechanical Fabry—Perot Interferometer in ESA TRP&GSTP programs, and the UVIS spectrometer CCD and holographic grating activities of GOMOS onboard ESA ENVISAT. He is the author or coauthor of more than 13 publications and four patents. His interests include scientific CCD sensors and their electronics, digital aerial cameras, and MOEMS applications.